An Energy Autonomous and Battery-Free Plant’s Electrical Impedance Measurement System

An Energy Autonomous and Battery-Free Plant's Electrical Impedance Measurement System.

Stefano Calvo*, Mattia Barezzi*, Umberto Garlando*, Roberto La Rosa†, and Danilo Demarchi*
*Department of Electronics and Telecommunications, Politecnico di Torino, Torino, Italy
† STMicroelectronics, Catania, Italy

Email: stefano.calvo@polito.it

***Abstract*—Food production is one of the main contributors to climate change and its impact is set to increase due to population growth. Smart agriculture aims at providing solutions to reduce food production and environmental impact while, at the same time, increasing crop production. This paper proposes a system based on STDES-BTAG01 by STMicroelectronics to monitor in-vivo stem electrical impedance, which is a parameter that has recently demonstrated its efficacy in assessing information about plants' water stress status. The developed system is completely battery-free and equipped with a wireless communication module to transmit the acquired data. It is powered by a small amorphous solar cell and transmits data to a base station exploiting the Bluetooth Low Energy (BLE) protocol. The system monitors the needed time to discharge a capacitor through the plant stem. After this, this span of time is used to compute the stem electrical impedance. Tests showed reading errors lower than 15% when dealing with impedance modules up to 180 kΩ. System characteristics (energy self-sufficiency, compactness, and low-power consumption) make the system implementable in the fields.**

***Index Terms*—Smart Agriculture, Water Stress, Stem Electrical Impedance, Plants' Resilience**

I. Introduction

Agricultural activity is one of the main contributors to climate change. It is responsible for more than a quarter of the total greenhouse gases emission and around 70% of the freshwater used worldwide [1]. Its impact is going to increase in the near future. Even though the world population growth rate has declined over the last decades, the number of people living on the planet is destined to reach more than 10 billion by the end of this century [2]. Climate change and unwise agricultural practices are leading to arable land reduction [3] and degradation [4], meaning that humanity has to rely on a reduced amount of arable lands whose yields are decreasing to feed an increasing world population. Smart agriculture aims to address this issue by merging farming and engineering knowledge to reduce food production footprint and, at the same time, increase crop productivity without excessively depleting the available resources. One of the most common approach to pursue these objectives is environmental monitoring, which gathers information by inspecting the environment surrounding crops [5]–[7] to help farmers make decisions by monitoring parameters such as temperature and soil humidity or performing weather forecasts. Although this method is widely implemented, researchers found that it may provide misleading or incomplete information [8], [9]. Indeed, *Garlando et al.* demonstrated that plants might suffer even if subjected to an optimal environment. In this case, environmental monitoring sensors may be unable to detect crop issues. In recent years, to overcome this limit, researchers developed techniques and devices to inspect crops themselves directly. For example, evapotranspiration has been inspected with a clip-shaped sensor directly clamped to leaves [10]. Moreover, stems and leaves growth rates have been monitored with sensors relying on a *Bragg*'s grating [11] and a strain gauge [12], respectively. Crops' water stress status has recently been monitored by inspecting the variations of the electric potential among plants and the compound where they are growing [13]. Another parameter to assess information regarding this key parameter is stem electrical impedance [14]–[16]. It has been demonstrated that plants' trunks and stems are electrically conductive [17], and their impedance variation provide valuable information regarding crops' water stress status [8]. This work presents a novel approach to inspect a plant's electrical impedance by exploiting the system proposed by *La Rosa et al.* [18] based on the energy-autonomous and battery-free wireless sensor platform with Bluetooth Low Energy (BLE) connectivity STDES-BTAG01 provided by STMicroelectronics.

The paper is organized as follows: Section II describes the implemented experimental setup, Sections III and IV show and analyze the results obtained during experiments, while section V concludes the article.

II. Experimental Setup

The purpose of the system is to measure the electrical resistance of the plant stem for very low frequencies, ideally performing the measurement in direct current (0 Hz).

The system embeds uniquely off-the-shelf devices mounted on a Printed Circuit Board (PCB). It consists of a STDES-TBAG01 board that embeds a Microcontroller Unit (MCU), in particular a STM32L0 by STMicroelectronics, a BLE module (BLUENRG-M2SP by STMicroelectronics) [19], an amorphous silicon solar cell (AM-1606C by Panasonic [20]), and a pass transistor (a SiP32432 by Vishay Siliconix). This latter has been chosen since it is turned on when a low input voltage is applied to its control pin. Fig. 1 shows the circuit connections and setup.

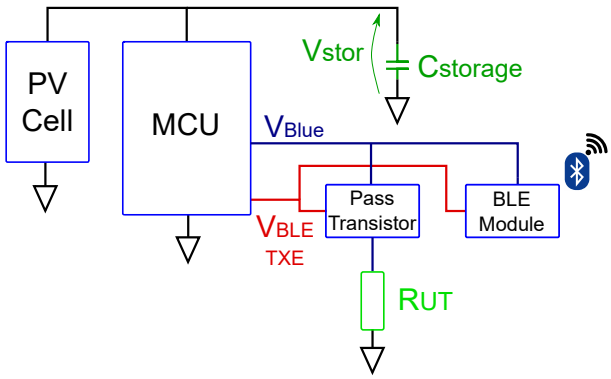

Fig. 1. Circuit schematics. R_{ut} is the resistance under test, $C_{storage}$ is a 440 µF storage capacitance, V_{BLE_TXE} is the control signal used to select if the BLE works in receiving mode (when pulled down) or transmitting mode (when pulled up), and V_{Blue} is the voltage used to power the BLE module and the resistance under test.

The embedded MCU ensures a wide range of supply voltage and input/output voltage that it can handle. They span from a minimum of 1.8 V to a maximum of 3.6 V. The system relies only on the internal LDO (Low-Dropout) regulator integrated into the MCU to minimize the power consumption, reduce the Bill Of Material (BOM), and optimize the system footprint. Therefore, no external voltage regulator or power management system are used to supply the remaining part of the circuit from the photovoltaic cell. Indeed, the whole system works with unregulated and time-varying supply voltage.

The measurement routine comprises the following three phases: Charging Phase, Measurement Phase, and Transmission Phase. The two latter ones are alternated cyclically in sequence.

- *Charging Phase*: the energy provided by the solar cell charges a 440 µF storage capacitor $C_{storage}$ up to a voltage value V_h equal to 3 V. During this phase, the MCU is in ultra-low power Stop Mode, the BLE module is off and unbiased, and the pass transistor is off.
- *Measurement Phase*: this phase starts when the voltage V_{stor} reaches the voltage value V_h and the MCU is woken up by an interrupt generated by the Power Voltage Detector (PVD). Since the pass transistor is piloted by the V_{BLE_TXE} signal it is turned on during this phase, and the BLE module is configured in receiver mode (RX). This configuration increases the overall MCU current consumption I_{MCU} so that $I_{MCU} > I_{pv}$ (where I_{pv} is the current provided by the solar cell) and it allows the storage capacitor to discharge. The storage capacitor $C_{storage}$ discharges both through the MCU and the resistance under test R_{ut} until the voltage V_{stor} reaches the value V_l equal to 2.6 V. The R_{ut} value is indirectly evaluated by measuring the time t_{meas} that takes the storage capacitance to discharge from the voltage value V_h to the voltage value V_l.
- *Transmission Phase*: the time t_{meas}, previously measured by the MCU, is transmitted via BLE protocol to a Base Station (BS). During this phase, the pass transistor is off, the MCU wakes up in run mode and it powers the BLE module in trasmitting mode.

Fig. 2 shows the timing evolution of the measurement routine.

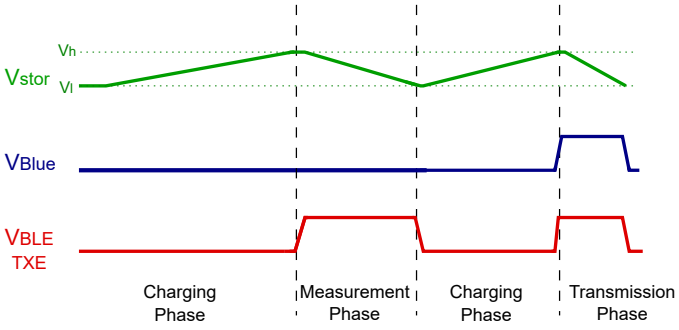

Fig. 2. Measurement timing schematics. V_{Blue} and V_{BLE_NRST} low levels are equal to 0 V while when they are high they are equal to V_{stor}.

The MCU measures the time t_{meas} by activating the Ultra-Low-Power Timer (LPTIM) with a resolution of 3.45 ms. This choice allows the lowest power consumption while the MCU performs the resistance measurement.

III. Measurements and Results

The time t_{meas} can be evaluated as in Eq. (1):

$$t_{meas} = R_{eq} \cdot C_{storage} \cdot ln\left(\frac{V_h}{V_l}\right) \tag{1}$$

where R_{eq} is the equivalent resistance that effectively discharges the $C_{storage}$ capacitor during the measurement phase, and the voltages V_{Blue} and V_{stor} are short-circuited through the high side transistor of a General Purpose Input Output (GPIO) circuit of the MCU with a negligible on resistance ($\approx$ 180 mΩ) compared to the R_{ut} resistance to be measured. Therefore the equivalent resistance R_{eq} can be expressed as in Eq. (2):

$$R_{eq} = R_{ut} || R_{sys} \tag{2}$$

R_{sys} considers the impedance due to the MCU and BLE circuitry. As a first order approximation R_{sys} can be expressed by Eq. (3):

$$R_{sys} \simeq \frac{V_h + V_l}{2} \cdot \frac{1}{I_{MCU} - I_{pv}} \tag{3}$$

As shown by Eq. (3), R_{sys} depends on two quantities that can not be known a priori. The current I_{MCU} consumed by the MCU can be estimated, but its instantaneous value is unknown, and the photo-current I_{pv} is highly dependent on the environmental light. Therefore, to take into account these effects, equation (1) can be rewritten as Eq. (4):

$$t_{meas} = C_{storage} \cdot (R_{ut} || R_{sys}) \cdot ln\left(\frac{V_h}{V_l}\right) \tag{4}$$

System input resistance, the parameter that takes into account the instantaneous MCU current consumption and solar

cell charging effect, has been compensated by performing multiple measurements with a stable light source (the same used for the other measurements) and without a load connected to the pass transistor: $R_{ut} \to \infty$ and $R_{eq} = R_{sys}$. Therefore, the relation holding between the resistance R_{ut} and the discharging time t_{meas} can be expressed by Eq. (5):

$$R_{ut} = A \cdot \frac{t_{oc} \cdot t_{meas}}{C_{storage} \cdot (t_{oc} - t_{meas})} \tag{5}$$

Where t_{oc} is the average time needed for discharging the capacitor with $R_{ut} \to \infty$ (compensating the system resistance contribution), A is a parameter extracted through the calibration of the system, to compensate the solar cell charging effect, and t_{meas} is the measured discharging time. This parameter was found to be dependent on the measured time t_{meas} and t_{oc} as expressed in Eq, (6).

$$A = \frac{34.5}{221.6 - 2.2 \cdot ((t_{meas}/t_{oc}) - 39)}(a.u.) \tag{6}$$

Exploiting equation 5, the results reported in Fig. 3 have been obtained. Results refer to measurements carried on with ceramic resistances.

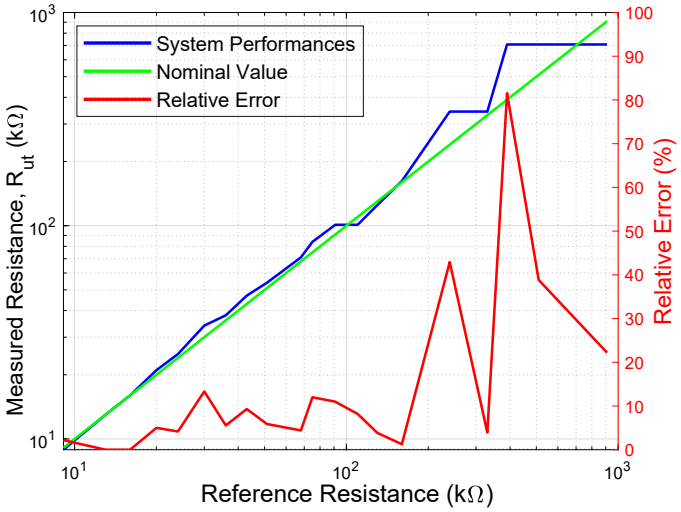

Fig. 3. R_{ut} measurement in the range from 0 Ω to 1000 kΩ. The green line represents the nominal resistance value, the blue line represents the resistance evaluated with the system, and the red line represents the absolute reading error.

IV. Data Analysis

The experimental results reported in Fig. 3 show that low resistance values are read more precisely than higher ones and that it is not possible to distinguish values higher than 180 kΩ. The main source of error is due to the system resistance R_{sys}. Its contribution is responsible for the 200 kΩ limitation. Despite the compensation discussed in Section III, the system resistance is still present in every measurement. When the resistance under test is significantly higher than the system resistance, the equivalent resistance of Eq. 2 is not affected by R_{ut}. It will result being equal to the system resistance. Therefore, higher resistance values will be masked because of they are in parallel with the system resistance R_{sys}. Another error source is the one responsible, for example, for the higher relative error during the 240 kΩ reading with respect to the 330 kΩ reading despite the latter has a higher value. The discharging time is read with an MCU able to discern finite amounts of elapsed timer periods only (3.45 ms). Therefore, the system's performance deteriorates when the needed time to discharge the capacitor between V_h and V_l falls between two consecutive timer periods. However, R_{ut} lower than 200 kΩ have been read with a maximum relative error of 13%, while the ones between 180 kΩ and 400 kΩ with a relative error up to 80% mainly due to the time discretization error. A higher resistance reading error overcomes the 100% relative error. Fig. 4 shows the device performance for resistance lower than 180 kΩ. This detection limit should not be an issue when dealing with plants. In fact, studies regarding in-vivo stem electrical impedance have shown that at low frequencies its modulus is in the order of few tens of kΩ [8].

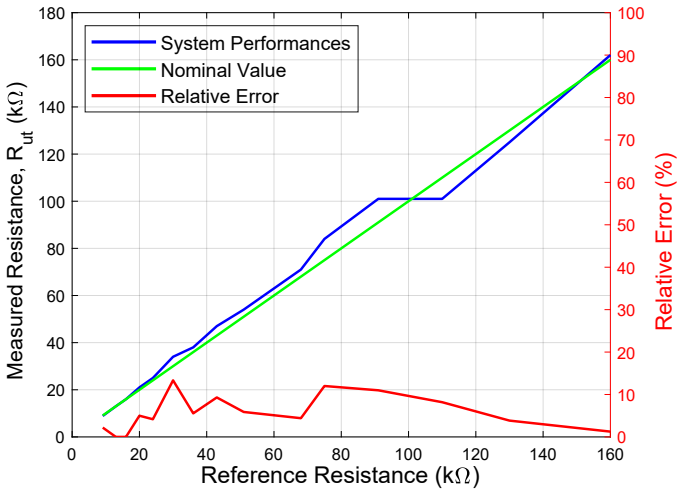

Fig. 4. R_{ut} measurement in the range from 0 Ω to 180 kΩ. The green line represents the nominal resistance value, the blue line represents the resistance evaluated with the system, and the red line represents the relative reading error.

V. Conclusions

This work paves the way towards a novel approach to inspect in-vivo plant stem electrical impedance in DC. The developed system to perform measurement is energetically autonomous and battery-free. It embeds the BLE wireless communication protocol to transmit data to a base unit where they are collected and analyzed. System characteristics offer the possibility of substituting complex, expensive, and hard-to-use systems used to perform in-vivo stem electrical impedance measurements. Preliminary results involving ceramic resistances show excellent accuracy when dealing with impedance modules lower than 180 kΩ with a maximum relative error of 13%. Future works will aim at improving the overall reading accuracy by decreasing the timer period used to monitor the storage capacitor discharging time and by improving the

management of the R_{sys} and I_{pv} contributions by performing an open-circuit supercapacitor discharge before every stem impedance measurement.

ACKNOWLEDGEMENT

This study was carried out within the Agritech National Research Center and received funding from the European Union Next-GenerationEU (PIANO NAZIONALE DI RIPRESA E RESILIENZA (PNRR) – MISSIONE 4 COMPONENTE 2, INVESTIMENTO 1.4 – D.D. 1032 17/06/2022, CN00000022). This manuscript reflects only the authors' views and opinions, neither the European Union nor the European Commission can be considered responsible for them.

REFERENCES

[1] H. Ritchie, P. Rosado, and M. Roser, "Environmental impacts of food production," *Our World in Data*, 2022, https://ourworldindata.org/environmental-impacts-of-food.

[2] H. Ritchie, L. Rodés-Guirao, E. Mathieu, *et al.*, "Population growth," *Our World in Data*, 2023, https://ourworldindata.org/population-growth.

[3] A. Burrell, J. Evans, and M. De Kauwe, "Anthropogenic climate change has driven over 5 million km2 of drylands towards desertification," *Nature communications*, vol. 11, no. 1, p. 3853, 2020.

[4] A. Alam, "Soil degradation: A challenge to sustainable agriculture," *International Journal of Scientific Research in Agricultural Sciences*, vol. 1, no. 4, pp. 50–55, 2014.

[5] N. Suma, S. R. Samson, S. Saranya, G. Shanmugapriya, and R. Subhashri, "Iot based smart agriculture monitoring system," *International Journal on Recent and Innovation Trends in computing and communication*, vol. 5, no. 2, pp. 177–181, 2017.

[6] S. Tenzin, S. Siyang, T. Pobkrut, and T. Kerdcharoen, "Low cost weather station for climate-smart agriculture," in *2017 9th international conference on knowledge and smart technology (KST)*, IEEE, 2017, pp. 172–177.

[7] T. Kasama, T. Koide, W. P. Bula, Y. Yaji, Y. Endo, and R. Miyake, "Low cost and robust field-deployable environmental sensor for smart agriculture," in *2019 2nd International Symposium on Devices, Circuits and Systems (ISDCS)*, IEEE, 2019, pp. 1–4.

[8] U. Garlando, S. Calvo, M. Barezzi, A. Sanginario, P. M. Ros, and D. Demarchi, "Ask the plants directly: Understanding plant needs using electrical impedance measurements," *Computers and Electronics in Agriculture*, vol. 193, p. 106 707, 2022.

[9] F. Cum, S. Calvo, D. Demarchi, and U. Garlando, "Machine learning models comparison for water stress detection based on stem electrical impedance measurements," in *2023 IEEE Conference on AgriFood Electronics (CAFE)*, 2023, pp. 108–112. DOI: 10.1109/CAFE58535.2023.10291805.

[10] V. Palazzari, P. Mezzanotte, F. Alimenti, F. Fratini, G. Orecchini, and L. Roselli, "Leaf compatible "eco-friendly" temperature sensor clip for high density monitoring wireless networks," *Wireless Power Transfer*, vol. 4, no. 1, pp. 55–60, 2017.

[11] D. Lo Presti, S. Cimini, C. Massaroni, *et al.*, "Plant wearable sensors based on fbg technology for growth and microclimate monitoring," *Sensors*, vol. 21, no. 19, p. 6327, 2021.

[12] Y. Zhao, S. Gao, J. Zhu, *et al.*, "Multifunctional stretchable sensors for continuous monitoring of long-term leaf physiology and microclimate," *ACS omega*, vol. 4, no. 5, pp. 9522–9530, 2019.

[13] D. Tran, F. Dutoit, E. Najdenovska, *et al.*, "Electrophysiological assessment of plant status outside a faraday cage using supervised machine learning," *Scientific reports*, vol. 9, no. 1, p. 17 073, 2019.

[14] U. Garlando, L. Bar-On, P. M. Ros, *et al.*, "Towards optimal green plant irrigation: Watering and body electrical impedance," in *2020 IEEE International Symposium on Circuits and Systems (ISCAS)*, IEEE, 2020, pp. 1–5.

[15] U. Garlando, L. Bar-On, P. M. Ros, *et al.*, "Analysis of in vivo plant stem impedance variations in relation with external conditions daily cycle," in *2021 IEEE International Symposium on Circuits and Systems (ISCAS)*, IEEE, 2021, pp. 1–5.

[16] S. Calvo, M. Barezzi, D. Demarchi, and U. Garlando, "In-vivo proximal monitoring system for plant water stress and biological activity based on stem electrical impedance," in *2023 9th International Workshop on Advances in Sensors and Interfaces (IWASI)*, IEEE, 2023, pp. 80–85.

[17] P. M. Ros, E. Macrelli, A. Sanginario, Y. Shacham-Diamand, and D. Demarchi, "Electronic system for signal transmission inside green plant body," in *2019 IEEE International Symposium on Circuits and Systems (ISCAS)*, IEEE, 2019, pp. 1–5.

[18] R. La Rosa, C. Dehollain, A. Burg, M. Costanza, and P. Livreri, "An energy-autonomous wireless sensor with simultaneous energy harvesting and ambient light sensing," *IEEE Sensors Journal*, vol. 21, no. 12, pp. 13 744–13 752, 2021.

[19] STMicroelectronics, "Bluerng-m2sp very low power application processor module for bluetooth low energy v5.0," STMicroelectronics Geneva,Switzerland, Tech. Rep., 2010. [Online]. Available: https://www.st.com/resource/en/datasheet/bluenrg-m2.pdf.

[20] Panasonic, "Amorton solar cell catalog," Tech. Rep., 2019. [Online]. Available: https://industry.panasonic.eu/products/energy-building/amorphous-solar-cells?langreferrer=panasonic-electric-works.com.